Received January 2002
Revised May 2003
Accepted May 2003

Numerical simulation of inductively coupled plasma flows under chemical non-equilibrium

Gérard Degrez and David Vanden Abeele
von Karman Institute for Fluid Dynamics (VKI), Rhode St-Gense, Belgium
Service de Mécanique des Fluides, Université Libre de Bruxelles (ULB), Bruxelles, Belgium
Paolo Barbante
von Karman Institute for Fluid Dynamics (VKI), Rhode St-Gense, Belgium
Dipartimento di Matematica, Politecnico di Milano, Milano, Italy
Benot Bottin
von Karman Institute for Fluid Dynamics (VKI), Rhode St-Gense, Belgium
Institut Suprieur Industriel de Bruxelles (ISIB), Bruxelles, Belgium

Keywords *Numerical analysis, Plasma physics, Flow, Equilibrium methods*

Abstract *This paper presents a detailed review of the numerical modeling of inductively coupled air plasmas under local thermodynamic equilibrium and under chemical non-equilibrium. First, the physico-chemical models are described, i.e. the thermodynamics, transport phenomena and chemical kinetics models. Particular attention is given to the correct modelling of ambipolar diffusion in multi-component chemical non-equilibrium plasmas. Then, the numerical aspects are discussed, i.e. the space discretization and iterative solution strategies. Finally, computed results are presented for the flow, temperature and chemical concentration fields in an air inductively coupled plasma torch. Calculations are performed assuming local thermodynamic equilibrium and under chemical non-equilibrium, where two different finite-rate chemistry models are used. Besides important non-equilibrium effects, we observe significant demixing of oxygen and nitrogen nuclei, which occurs due to diffusion regardless of the degree of non-equilibrium in the plasma.*

The second author was supported by a grant from the Flemish Institute for the Promotion of Scientific-Technological Research in the Industry (IWT). The third author was supported by a Marie Curie Grant in the TMR program of the European Union. This work was partially supported by the INTAS Research Grant RFBR-95-1329 and benefited from fruitful discussions with Project Coordinator Dr G.S.R. Sarma (DLR, Germany) and Project partner Dr A.F. Kolesnikov (Institute for Problems in Mechanics, Moscow).

International Journal of Numerical Methods for Heat & Fluid Flow
Vol. 14 No. 4, 2004
pp. 538-558

0961-5539
DOI 10.1108/09615530410532286

1. Introduction

During their entry in atmosphere, space (re-)entry vehicles, whether manned such as the space shuttle or unmanned such as planetary probes, are exposed to very high temperature flows and are therefore protected against excessive heating by heat shields made out of thermal protection materials (TPMs). Before their actual use in space vehicles, the performance of TPMs must be tested in ground facilities. It is precisely for this purpose that the European Space Agency recently financed, together with the Belgian Federal Office of Scientific, Technical and Cultural affairs, the construction at the von Karman Institute (VKI) of a large scale (1.2 MW) inductively coupled plasma (ICP) flow wind tunnel (Plasmatron) (Bottin *et al.*, 1999a).

In this kind of facility (Figure 1), the operating gas (air or any other mixture of gases reproducing a particular planetary atmosphere) is heated in an electrodeless manner to a partially ionized plasma state with peak temperatures around 10,000 K. The gas is injected into a quartz tube surrounded by a copper inductor. A radio-frequency electrical current runs through the inductor and induces a secondary current through the gas inside the quartz tube, which heats up by means of ohmic dissipation.

A key characteristic of TPMs is their catalytic properties. For a given wall temperature and free stream properties (total enthalpy, pressure and velocity), the wall heat flux can depend strongly on the wall catalycity if the boundary layer developing around the body is far from chemical equilibrium. Contrary to arc heated wind tunnels, in which the flow is polluted by metallic impurities produced by electrode erosion, inductively heated wind tunnels produce plasma jets of high chemical purity and are therefore, particularly, suited for the determination of material catalycity.

Except in very special conditions (e.g. at very low pressures), material catalycity cannot be measured directly, but has to be determined indirectly

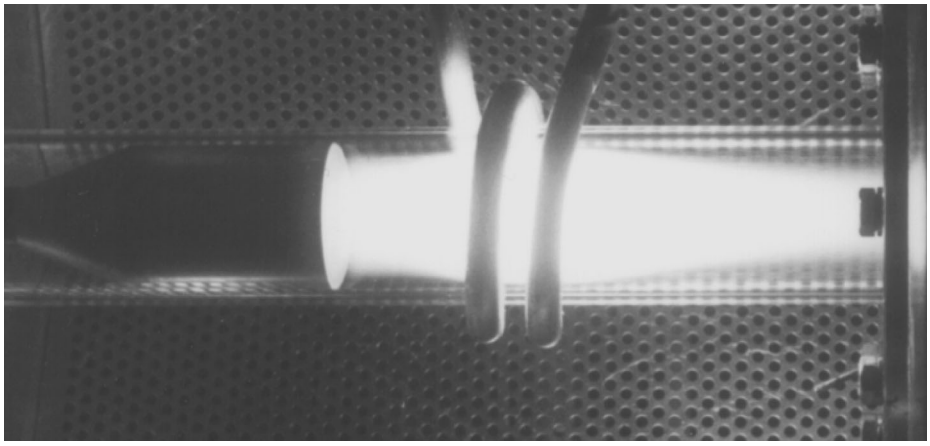

Figure 1.
Small ICP torch in operation (VKI mini-torch, argon, 1 atm, 3 kW, 27 MHz)

through its effect on wall heat flux. A methodology to determine wall catalycity, which relies on both experimental and computational results, has been developed by Russian researchers (Kolesnikov, 1999; Kolesnikov *et al.*, 1998). The implementation of this methodology at the VKI has motivated the development of a series of computational tools for the simulation of inductively coupled plasma flows and hypersonic (re-)entry flows, to be used in conjunction with experimental techniques for the characterization of the flow in the VKI Plasmatron and of TPM catalycity. This paper describes the developed numerical model of high-pressure air ICPs under local thermodynamic equilibrium (LTE) and under chemical non-equilibrium (but at thermal equilibrium).

Air ICPs under LTE have been intensively studied by Vasil'evskii *et al.* (1996). Models of high-pressure ICPs under both thermal and chemical non-equilibrium have been presented earlier by Benoy (1993), Kulumbaev (1999), Mostaghimi *et al.* (1987) and Semin (1991). However, these models only dealt with the relatively straightforward case of argon plasmas and cannot be easily extended to more complex mixtures, such as air, for two main reasons. First, the modeling of thermodynamic and transport phenomena in multi-component molecular plasmas is considerably more complex than for argon, which is a three-component (Ar, Ar^+, e^-) atomic plasma. In particular, one should provide an adequate model of diffusion processes between the numerous species in the plasma. Secondly, when switching from argon to molecular plasmas, the increased number of species and the need to include stiff chemistry drives up the computational cost of the numerical simulations. To obtain converged results in reasonable computation times, the use of efficient iterative methods then becomes essential.

2. Governing equations

ICP flows can be described by an axisymmetric model in which the outer inductor is modelled by a series of parallel current-carrying rings, assumed infinitely thin for simplicity (Figure 2). The governing equations consist of the conservation equations of gas dynamics supplemented by a magnetohydrodynamic induction equation for the induced electric field.

2.1 Conservation equations of gas dynamics

Despite small amplitude oscillations due to the high frequency electromagnetic (EM) field, ICP flows may be considered quasi-steady (Vanden Abeele and Degrez, 2000). Indicating the axial, radial and azimuthal coordinates by, respectively, z, r and θ, the set of conservation equations may be written in a compact axisymmetric form:

$$\frac{\partial(r\mathbf{F}^{c})}{\partial z}+\frac{\partial(r\mathbf{G}^{c})}{\partial r}=\frac{\partial(r\mathbf{F}^{d})}{\partial z}+\frac{\partial(r\mathbf{G}^{d})}{\partial r}+\mathbf{S}, \tag{1}$$

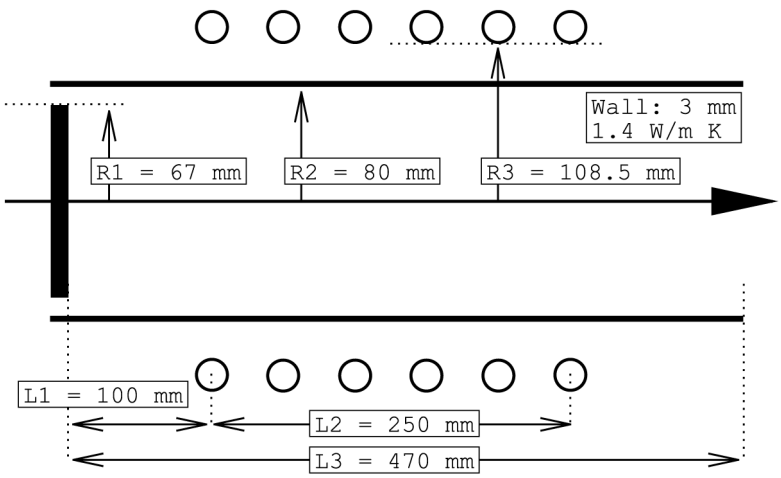

Figure 2.
VKI plasmatron torch geometry

where $\mathbf{F}^{c}$, $\mathbf{G}^{c}$ and $\mathbf{F}^{d}$, $\mathbf{G}^{d}$ are the convective and diffusive fluxes, respectively, and $\mathbf{S}$ represents the source terms in the equations. Because ICP flows are characterized by low Mach numbers ($M < 0.1$), we may neglect the contribution of kinetic energy (negligible with respect to the plasma enthalpy) as well as the work of the shear stresses (negligible with respect to the heat fluxes). Since Reynolds numbers are low as well ($Re \sim 500$), the flow field is laminar and no modelling of turbulence is needed. Assuming thermal equilibrium (single temperature problem), then the precise expressions of the various fluxes are:

$$\mathbf{F}^{c} = (\rho u, \rho y_s u, \rho u^2 + p, \rho uv, \rho uw, \rho uh)^t \tag{2}$$

$$\mathbf{G}^{c} = (\rho v, \rho y_s v, \rho uv, \rho v^2 + p, \rho vw, \rho vh)^t \tag{3}$$

$$\mathbf{F}^{d} = \left(0, -J_{zs}, \tau_{zz}, \tau_{zr}, \tau_{z\theta}, -\sum_{s=1}^{n_s} J_{zs} h_s - q_z\right)^t \tag{4}$$

$$\mathbf{G}^{d} = \left(0, -J_{rs}, \tau_{zr}, \tau_{rr}, \tau_{r\theta}, -\sum_{s=1}^{n_s} J_{rs} h_s - q_r\right)^t \tag{5}$$

$$\mathbf{S} = (0, r\dot{m}_s, rF_z, p + \rho w^2 - \tau_{\theta\theta} + rF_r, -\rho vw + \tau_{r\theta}, r\dot{Q})^t, \tag{6}$$

where ρ is the global density, y_s the species mass fractions ($s = 1, \ldots, n_s$), p the pressure, u, v and w the axial, radial and azimuthal velocity components, h the internal enthalpy, $\vec{J}_s$ the diffusive mass flux of species s, h_s the species

enthalpies per unit mass, τ_{ij} the viscous stresses, $\vec{q}$ the conduction heat flux, $\dot{m}_s$ the chemical source terms, and $\vec{F}$ and $\dot{Q}$ are the body force and volume heat sources/sinks, respectively, which are specified in Section 2.2 (equation (11)). While the considered flows are axisymmetric, they may contain a significant amount of "swirl" (transverse velocity component w), which serves to stabilize the flow field.

The shear stresses may be further expressed as

$$\begin{aligned}
&\tau_{zz} = \mu\left(2\frac{\partial u}{\partial z} - \frac{2}{3}\nabla\cdot\vec{u}\right) \quad \tau_{zr} = \mu\left(\frac{\partial u}{\partial r} + \frac{\partial v}{\partial z}\right) \quad \tau_{rr} = \mu\left(2\frac{\partial v}{\partial r} - \frac{2}{3}\nabla\cdot\vec{u}\right)\\
&\tau_{z\theta} = \mu\frac{\partial w}{\partial z} \quad \tau_{r\theta} = \mu\left(\frac{\partial w}{\partial r} - \frac{w}{r}\right) \quad \tau_{\theta\theta} = \mu\left(2\frac{v}{r} - \frac{2}{3}\nabla\cdot\vec{u}\right)\\
&\nabla\cdot\vec{u} = \frac{\partial u}{\partial z} + \frac{\partial v}{\partial r} + \frac{v}{r},
\end{aligned} \tag{7}$$

where Stokes' hypothesis has been used, and the heat flux vector components are expressed as

$$q_z = -\kappa\frac{\partial T}{\partial z} \quad q_r = -\kappa\frac{\partial T}{\partial r}. \tag{8}$$

The expression for the diffusion fluxes $\vec{J}_s$ is discussed later (equation (15)). The source term $\dot{Q}$ may be decomposed into a Joule heating term and a radiative cooling term ($\dot{Q} = \dot{Q}_{\text{Joule}} - \dot{Q}_{\text{rad}}$, assuming optically thin radiation). For the air ICP flows at subatmospheric pressures considered in this paper, radiative losses can be safely neglected (Dresvin *et al.*, 1977).

In order to close the system of governing equations, a set of thermodynamic, transport and chemical kinetics models are required. These models, which are to be described in Sections 3-5, have been implemented in a common software library (PEGASE) used by all VKI high-temperature CFD solvers (Bottin *et al.*, 1999b).

2.2 Magnetohydrodynamic induction equation

Owing to the axial symmetry of the problem, all electromagnetic phenomena may be expressed in terms of the azimuthal electric field, which consists of a single Fourier mode:

$$\vec{E} = E\exp(\mathrm{i}2\pi ft)\vec{e}_\theta, \tag{9}$$

where f represents the operating frequency of the torch. To consider phase-differences within the plasma, the electric field amplitude $E(r,z)$ stands for a complex variable. The electric field amplitude can be shown to satisfy the following fully resistive axisymmetric MHD induction equation, both inside the

torch and on a far field domain which covers the space around the torch (Mekideche, 1993):

$$\frac{\partial^2 E}{\partial z^2} + \frac{1}{r}\,\frac{\partial}{\partial r}\left(r\,\frac{\partial E}{\partial r}\right) - \frac{E}{r^2} - \mathrm{i}2\pi\mu_0\sigma f\,E = -\mathrm{i}\mu_0 2\pi f \sum_{j=1}^{n_c} \delta(\vec{r} - \vec{r}_j) I_{\mathrm{C}}, \quad (10)$$

where σ is the electrical conductivity of the plasma. The Dirac δ distribution in the right hand side takes care of the singular current density in the n_c (infinitely thin) inductor rings. For the radio-frequency currents used in high-pressure ICPs, it is reasonable to assume that a single coil current with amplitude I_{C} oscillates at phase angle zero through each coil ring (Jaeger *et al.*, 1995). The electric currents in the ICP are generating Lorentz body forces and Joule heat sources in the gas dynamics equations (equation (6)), whose expression is (Vanden Abeele and Degrez, 2000):

$$\begin{aligned} F_r &= \frac{\sigma}{4\pi f}\left(\frac{E_{\mathrm{R}}}{r}\,\frac{\partial r E_{\mathrm{I}}}{\partial z} - \frac{E_{\mathrm{I}}}{r}\,\frac{\partial r E_{\mathrm{R}}}{\partial z}\right) \\ F_z &= \frac{\sigma}{4\pi f}\left(\frac{E_{\mathrm{R}}}{r}\,\frac{\partial r E_{\mathrm{I}}}{\partial r} - \frac{E_{\mathrm{I}}}{r}\,\frac{\partial r E_{\mathrm{R}}}{\partial r}\right) \\ \dot{Q}_{\mathrm{Joule}} &= \frac{\sigma}{2}\left(E_{\mathrm{R}}^2 + E_{\mathrm{I}}^2\right), \end{aligned} \quad (11)$$

where E_{R} and E_{I} are the real and imaginary parts of the electric field amplitude.

3. Modeling of thermodynamic properties

In the present computational models, we consider mixtures of thermally perfect gases in thermal equilibrium for which the pressure is related to the temperature and the species densities by Dalton's law

$$p = \sum_{s=1}^{n_s} \rho y_s R_s T. \quad (12)$$

The other required thermodynamic relation relates the internal energy to the species densities and temperature:

$$\tilde{\varepsilon} = \sum_{s=1}^{n_s} \rho y_s \varepsilon_s(T) \quad (13)$$

where $\tilde{\varepsilon}$ is the mixture internal energy per unit volume and $\varepsilon_{\mathrm{s}}(T)$ are the species internal energies per unit mass.

For monoatomic or diatomic species such as the major constituents of air between 250 and 15,000 K, the thermodynamic properties can be directly calculated from statistical mechanics (Anderson, 1989; Vincenti and Kruger, 1965), provided assumptions are made concerning the number of electronic

levels to be considered in the expressions, and the modelling of vibration/rotation coupling. Both issues were thoroughly investigated (Bottin *et al.*, 1999b). For each species under consideration, the influence of the number of electronic levels was assessed by comparing the computed enthalpies over the temperature range of interest for number of electronic levels within a reasonable range. Such a comparison is shown in Figure 3 for the N^+ ion. One observes that the curves corresponding to six or more electronic levels are superimposed, from which it is concluded that it suffices to take six electronic levels into account to accurately compute the thermodynamic properties of the N^+ ion. The number of levels to be considered for the constituents of the 13-species air model is given by Bottin *et al.* (1999b).

In the simplest (rigid rotator/harmonic oscillator) model for diatomic molecules, rotation and vibration energy modes are decoupled. In reality though, molecules stretch while rotating and vibrations alter the moment of inertia, so that rotation and vibration are coupled and should be treated together. First-order anharmonicity correction models which consider rotation/vibration (Mayer and Mayer, 1946) or full rotation/vibration/electronic (Drellishak *et al.*, 1965) coupling have been compared to literature data based on the direct summation method (Gurvich *et al.*, 1989), as shown in Figure 4 for the O_2 molecule (number of electronic levels ranging between 5 and 18). Although the full coupling model provides better agreement with literature data up to 8,000 K, it appears to be totally inadequate beyond this point. This phenomenon is due to the fact that the oxygen molecule has many excited levels in the low energy range. In contrast, for the nitrogen molecule, first-order corrections remain accurate up to 15,000 K. In any event, inaccuracies in the anharmonicity corrections are in practice unimportant because molecules

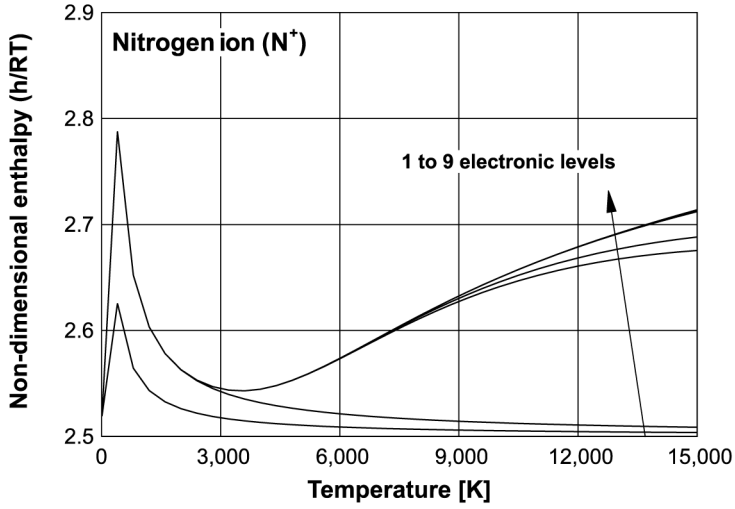

Figure 3.
Enthalpy of N^+ ion as a function of the number of electronic levels

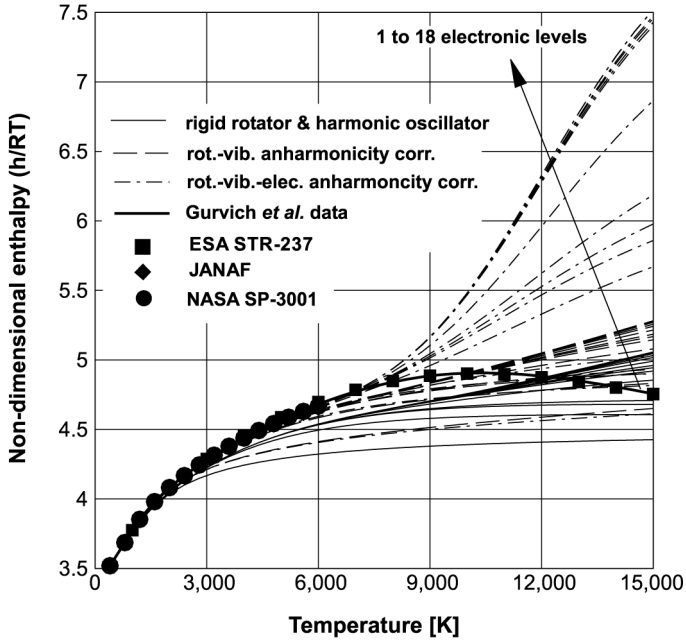

Figure 4.
Comparison of anharmonicity correction models for the O_2 molecule at 1 bar

dissociate at temperatures where the basic decoupled model is still accurate. As a result, the mass fraction of molecules and ionized molecules is so small at higher temperatures that inaccuracies in the anharmonicity corrections have essentially no influence on the computational results. In conclusion, it appears that the gain in accuracy of computed thermodynamic quantities provided by anharmonicity corrections does not justify the additional computational cost.

For equilibrium flows, the thermodynamic relations (12 and 13) are complemented by n_r equilibrium and n_c nuclei/charge conservation equations (with $n_r + n_c = n_s$) so that the number of independent thermodynamic variables reduces to two, e.g. pressure and temperature. The mixture composition is computed as a function of these independent variables using an original, partly analytical, partly numerical method based on a Schur-complement approach (Bottin *et al.*, 1999b). Basically, its principle is to solve for the logarithms of mass or mole fractions using a Newton iterative method. In terms of these variables, the equilibrium relations are *linear* so that n_r unknowns can be eliminated analytically, leaving only a system of n_c equations in n_c unknowns [1] to solve numerically. As the number of nuclei is much smaller than the number of species in complex gas mixtures such as air, the computational cost is dramatically reduced, which is an important feature for a CFD application since the composition calculation routine has to be called for each mesh point and at each iterative (time) step.

4. Modeling of transport phenomena

4.1 Transport coefficients

Transport properties are computed by the method of Chapman-Enskog as a function of the chemical composition, the temperature, pressure and the interaction potentials between the various colliding plasma particles (Hirschfelder *et al.*, 1967). The first-order correction to the equilibrium Maxwell-Boltzmann solution is obtained in terms of a series of Sonine polynomials. Usually, taking the first non-vanishing Sonine contribution in the expression for the transport coefficients provides sufficiently accurate results.

Whereas the expressions for binary diffusion coefficients are simple, the rigourous expressions for mixture transport properties such as viscosity and thermal conductivity derived by Hirschfelder *et al.* (1967) involve ratios of $n_s \times n_s$ determinants, and are consequently, prohibitively expensive for CFD applications. Therefore, approximations to these formulas, commonly referred to as mixture rules, have been derived by several researchers.

The accuracy of mixture rules for various transport properties has been investigated in detail (Bottin *et al.*, 1999b). For the viscosity, the mixture rule by Yos (1963) was found to provide accurate results. For the thermal conductivity, the heavy particles translational contribution was found to also be accurately evaluated by Yos' mixture rule, whereas the contribution of the internal degrees of freedom is adequately modelled by an Eucken-type approximation (Gupta *et al.*, 1990). To evaluate the electron contribution on the one hand, and all electron transport properties in general, higher order terms need to be kept in the expansion of Sonine polynomials. The formulas by Devoto (1967) and Kolesnikov and Tirsky (1984) with two non-vanishing Sonine polynomials were found to be equivalently accurate and efficient (Bottin *et al.*, 1999b). Finally, for equilibrium flows, the contribution to the heat flux due to the diffusion fluxes $\left(\sum_s \vec{J}_s h_s\right)$, which is spelled out for chemical non-equilibrium flows, can be conveniently modelled by means of a reactive thermal conductivity:

$$\sum_s \vec{J}_s h_s \approx -\nabla \cdot (\kappa_r \nabla T). \tag{14}$$

The above expression has been derived by Butler and Brokaw (1957) for neutral reactive gas mixtures, based on the assumption that no diffusion of elements ("demixing") occurs. It was shown (Bottin *et al.*, 1999b) that this expression is also valid for quasi-neutral mixtures of ionized gases under conditions of vanishing electric current. This expression was found to be more accurate than the mixture rule by Yos (1963) (see also Gupta *et al.*, 1990) when the degree of ionization is significant, as shown in Figure 5, which shows the various contributions to the thermal conductivity of equilibrium air up to 15,000 K. It is observed that the present results obtained using the expression by Butler and Brokaw are in excellent agreement with the results of

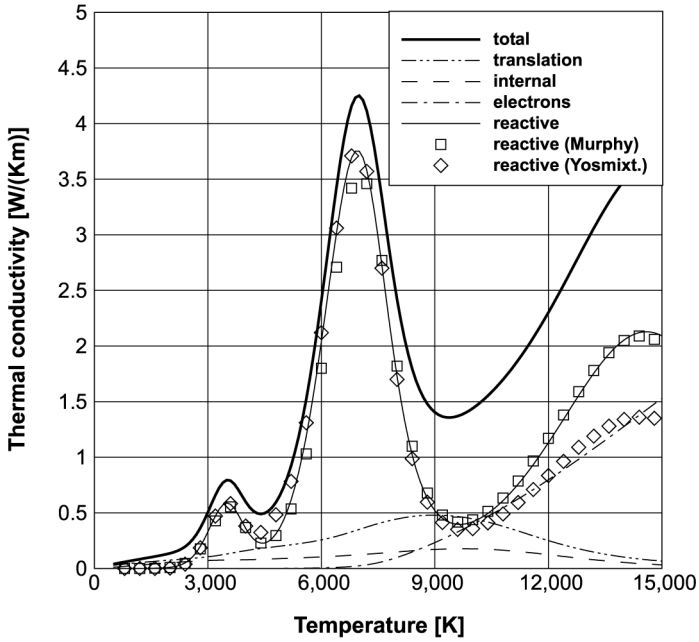

Figure 5.
Contributions to the thermal conductivity of equilibrium air at 1 atm

Murphy (1995) based on the rigourous expressions by Hirschfelder *et al.*, while Yos' mixture rule under-predicts the reactive thermal conductivity above 9,000 K.

The electrical conductivity, which is due entirely to the electrons, is accurately computed using the simplified expressions by Devoto (1967) or by Kolesnikov and Tirsky (1984).

4.2 Multi-component diffusion

Special care has been taken to the computation of the mass diffusion fluxes $\vec{J}_s$. These fluxes are commonly evaluated using the Fick's law approximation $\vec{J}_s = -\rho D_s \nabla c_s$, which has the advantage of an easy implementation, but violates mass conservation

$$\sum_s \vec{J}_s = 0.$$

In the present computational models, diffusion fluxes are evaluated using the full Stefan-Maxwell equations, which are equivalent to the Chapman-Enskog multi-component diffusion expressions (Hirschfelder *et al.*, 1967). Neglecting pressure and thermal diffusion as well as the effect of the magnetic field, we have

$$\frac{M}{\rho}\sum_{t=1}^{n_s}\left(\frac{x_s M_s \vec{J}_t - x_t M_t \vec{J}_s}{M_s M_t \mathscr{D}_{st}}\right) = \nabla x_s - \frac{\rho y_s \mathscr{Q}_s}{p}\vec{E}_{\text{amb}} \tag{15}$$

where M_s is the species molar masses, M the mixture molar mass, x_s the molar fractions, $\mathscr{D}_{st}$ the binary diffusion coefficients, and $\mathscr{Q}_s$ the species charge per unit mass. It can be proven that no net electric current flows in the poloidal (r, z) plane under conditions of thermal equilibrium (Vanden Abeele, 2000). The "ambipolar" electric field $\vec{E}_{\text{amb}}$ is then determined by imposing the additional constraint

$$\sum_{s=1}^{n_s} \mathscr{Q}_s \vec{J}_s = 0. \tag{16}$$

Equations (15) and (16) represent linear systems (one in each coordinate direction) in $n_s + 1$ unknowns, the diffusion fluxes and the ambipolar electric field, which are solved using an iterative method recently proposed by Sutton and Gnoffo (1998), adapted to the case of diffusion in ionized mixtures.

Different physics takes place in the azimuthal direction, where strong electric currents flow. Diffusion is driven by the induced electric field (equation (9)) rather than the ambipolar field and equation (15) simplify to Ohm's law

$$\mathscr{Q}_{\text{e}} \vec{J}_{\text{e}} = \sigma \vec{E}, \tag{17}$$

which has been used to derive equation (10).

5. Chemical reactions

Chemical source terms $\dot{m}_s$ are expressed according to the law of mass action, i.e.

$$\dot{m}_s = M_s \sum_{r=1}^{n_r} (\nu''_{sr} - \nu'_{sr}) \left\{ k_{\text{f}r} \prod_{t=1}^{n_s} \left(\frac{\rho_t}{M_t} \right)^{\nu'_{tr}} - k_{\text{b}r} \prod_{t=1}^{n_s} \left(\frac{\rho_t}{M_t} \right)^{\nu''_{tr}} \right\} \tag{18}$$

where n_r is the total number of reactions that involve species s, ν'_{sr} and ν''_{sr} are the stoichiometric coefficients for reactants and products, respectively, and $k_{\text{f}r}$ and $k_{\text{b}r}$ are the forward and backward reaction rates of reaction r. We recall that the previous expression is valid only if the n_r reactions considered are elementary reactions, i.e. reactions that take place in one single step. The forward reaction rates $k_{\text{f}r}$ are taken from Arrhenius data fits available in literature (Gnoffo *et al.*, 1989; Selle and Riedel, 2000). The backward reaction rates are computed from $k_{\text{f}r}$ and the equilibrium constant K_{cr}: $k_{\text{b}r} = k_{\text{f}r}/K_{cr}$. The equilibrium constant, which is related to the Gibbs free energy, is computed from statistical mechanics (Bottin *et al.*, 1999b) together with thermodynamic quantities.

6. Discretization and iterative solution procedure

6.1 Space discretization

The governing equations (1 and 10) are discretized using a co-located cell-centred finite volume method on structured meshes.

6.1.1 Gas dynamics equations. In ICP flowfields that are being characterized by low Mach numbers and therefore, low compressibility effects, the discrete equations are written in terms of the set of primitive variables $\mathbf{U} = (p, x_s, \rho\vec{u}, T)^t$. For such low speed flows, central discretizations on co-located grids are known to be subject to pressure stability problems. This is the reason why the vast majority of ICP models in the literature are based on a staggered grid arrangement. In the present study, we adopted a pressure-stabilized co-located grid approach (Ferziger and Perić, 1996) whose main advantage is a much simpler data structure.

Spurious pressure oscillations are suppressed in a conservative manner by adding a small dissipative pressure term to the convective mass flux, i.e. denoting the flowfield variables on both sides of a cell edge by the subscripts L and R, the pressure-stabilized normal mass flux at the cell edge (subscript E) is computed as

$$\tilde{f}_{m,E} = \frac{(\rho u_n)_L + (\rho u_n)_R}{2} - \frac{\Lambda}{\beta}(p_R - p_L) \tag{19}$$

where β is an estimate of the maximum velocity in the flow and Λ a factor to scale the pressure dissipation properly in regions of low cell Reynolds number:

$$\Lambda = \frac{\mathrm{Re}_h}{1 + \mathrm{Re}_h} \quad \mathrm{Re}_h = \frac{\rho\beta h}{\mu} \tag{20}$$

where h is some cell characteristic length. The previous definition indeed satisfies the asymptotic scalings $\Lambda/\beta \rightarrow h/\nu$ in the diffusion-dominated limit and $\Lambda/\beta \rightarrow 1/\beta$ in the advection-dominated limit.

At high Reynolds numbers, central discretizations also suffer from velocity oscillation problems. In the present model, these oscillations are controlled by introducing upwinding in the evaluation of the convective fluxes, i.e. the convective flux vector across the cell edge E with normal $\vec{n}$ is expressed as

$$\mathbf{F}_n^c = \left(\tilde{f}_{m,E}, \tilde{f}_{m,E} y_{s,E} \tilde{f}_{m,E} u_E + \frac{p_L + p_R}{2} n_x, \tilde{f}_{m,E} v_E + \frac{p_L + p_R}{2} n_y, \tilde{f}_{m,E} w_E, \tilde{f}_{m,E} h_E\right)^t \tag{21}$$

where for any quantity q

$$q_E = \frac{q_L + q_R}{2} - \mathrm{sign}\left(\tilde{f}_{m,E}\right) \frac{q_R - q_L}{2} \tag{22}$$

and $q_{L,R}$ are calculated from the neighbouring cell values using a linear or non-linear reconstruction (Hirsh, 1988). Non-linear positive reconstruction is needed for the energy and species mass fluxes whereas linear reconstruction is

sufficient for the momentum fluxes. Diffusive fluxes are computed using a central discretization.

6.1.2 MHD induction equation. The MHD induction equation (10) being linear, was found convenient to decompose the electric field between the contribution of the coil rings E_V, which can be computed analytically using the Biot-Savart law, and the plasma-induced part E_P (Vanden Abeele and Degrez, 2000). Substracting the equation for the contribution of the coil rings from equation (10), one then obtains the induction equation for the plasma contribution:

$$\frac{\partial^2 E_P}{\partial z^2} + \frac{1}{r}\frac{\partial}{\partial r}\left(r\frac{\partial E_P}{\partial r}\right) - \frac{E_P}{r^2} - \mathrm{i}2\pi\mu_0\sigma f(E_P + E_V) = 0. \tag{23}$$

A straightforward central discretization is sufficient to ensure numerical stability for this Helmholtz-type equation. Contrary to most existing high pressure ICP models, the induction equation is discretized on a far-field mesh which extends beyond the torch. The main advantage of this approach is the simple far-field boundary conditions which preserve the sparsity of the algebraic system, in contrast with the integral boundary condition used in most existing models (Vanden Abeele and Degrez, 2000; Van Dijk *et al.*, 2002).

6.2 Iterative solution strategy

To solve the discretized system of equations (1) and (23), we use a set of damped quasi-Newton strategies, together with a modern preconditioned Krylov subspace iterative technique (Saad, 1995), viz. the preconditioned GMRES algorithm, for the linear systems solved. The main reasons for selecting this type of iterative strategies lies in their ability to handle stiff systems and their fast iterative convergence, which is essential for the flow problems under consideration because of the high CPU cost per iteration associated to the evaluation of thermodynamic and transport properties.

In the initial iterations, a robust damped Picard strategy is used. Denoting by U and E the vectors of flowfield and EM variables, respectively, they are updated by solving separately the linear systems

$$J_P(U^{k+1} - U^k) = -R_U^k \tag{24}$$

$$J_E(E^{k+1} - E^k) = -R_E^k \tag{25}$$

where R_U and R_E are the space discretization residuals and J_E, J_P approximate jacobians. To ensure the robustness of the method, the flowfield jacobian is computed based on a first-order upwind reconstruction and by freezing the convective mass flux and ρ at iterative level k in the evaluation of the momentum, species and energy convective flux jacobians (Picard approximation). Specifically, at the interface between cells (i, j) and $(i + 1, j)$,

the convective flux jacobians of the terms $\tilde{f}_{m,E}q_E$ are approximated by (see equation (21))

$$\frac{\partial \tilde{f}_{m,EqE}}{\partial \mathbf{U}_{i,j}} \approx \frac{(1+\mathrm{sign}\tilde{f}_{m,E})}{2}\tilde{f}^{k}_{m,E}\left(\frac{\partial q}{\partial \mathbf{U}}\right)_{i,j}$$
$$\frac{\partial \tilde{f}_{m,EqE}}{\partial \mathbf{U}_{i+1,j}} \approx \frac{(1-\mathrm{sign}\tilde{f}_{m,E})}{2}\tilde{f}^{k}_{m,E}\left(\frac{\partial q}{\partial \mathbf{U}}\right)_{i+1,j} \quad (26)$$

Damping is, in general, necessary to ensure convergence. It is achieved by multiplying the diagonal entries in the Picard jacobian by a factor $(1 + 1/\mathrm{CFL})$ where the damping parameter CFL resembles the Courant number used in time-stepping schemes. Furthermore, solution updates are multiplied by an under-relaxation factor $\alpha = 0.7$.

Later, when the Picard method has converged around one order of magnitude, it switches to a damped quasi-Newton method, which differs from the Picard approach only by the evaluation of the flowfield jacobian. It is still computed based on a first-order reconstruction, but without freezing the convective mass flux, using a finite difference method.

The above Picard and quasi-Newton methods both solve for the flow and EM fields in a loosely coupled manner. A full Newton method, in which all equations are solved in a fully coupled manner, has also been considered. However, it was found that the important non-linear convergence gains obtained by full coupling are offset by a significant decrease in speed of convergence at the linear level (Vanden Abeele and Degrez, 2000).

7. Numerical results

7.1 ICP geometry, computation parameters

We simulate the heating chamber of the VKI Plasmatron wind tunnel (Bottin *et al.*, 1999a) to investigate the importance of chemical non-equilibrium effects in air ICPs. The problem geometry and operating conditions for the calculation are shown in Figure 2. Computations are performed using an 11-species air model (N_2, O_2, N, O, NO, NO^+, N^+, O^+, N_2^+, O_2^+, e^-). All thermodynamic and transport data (collision integrals) used for the simulations may be found in the work of Bottin (1999) and Vanden Abeele (2000). We model chemistry in the plasma in three different manners:

(1) assuming LTE, where we force the elemental composition plasma to be constant in space (79 per cent nitrogen, 21 oxygen elements per volume) by assuming vanishing nuclei diffusion fluxes (assumption also needed to apply equation (14));

(2) using the chemical kinetics model of Selle and Riedel (2000); and

(3) using the chemical kinetics model of Park as published by Gnoffo *et al.* (1989).

7.2 Convergence history

Calculations are run on a contemporary PC with a 900 MHz processor. A highly stretched 70×48 gas dynamics mesh and a 110×100 EM field mesh are used; an extensive mesh-refinement study has shown that this resolution is sufficient refined to obtain grid-converged results (Vanden Abeele *et al.*, 1999). The convergence history obtained for the calculations is shown in Figure 6. First, the LTE calculation is performed; after 50 Picard iterations, the quasi-Newton method is switched on and rapid convergence is observed. Next, the obtained LTE result serves as an initial solution for the subsequent non-equilibrium calculations. Usually, the LTE solution is sufficiently good to allow to immediately restart with the quasi-Newton method. The LTE calculations easily converge to machine accuracy; for the non-equilibrium calculations on fine meshes considered here, the residual norm is reduced by six orders of magnitude, after which convergence stagnates. We found that this convergence problem could be overcome by using lower values for the under-relaxation parameters CFL and α. For the LTE calculations, the required memory is 52 MB, where each iteration takes ~ 30 s; for the non-equilibrium calculations, 160 MB is needed and computation times increase sixfold to ~ 3 min per iteration.

7.3 Comparison of results

In Figures 7-9, we compare the computed results for the temperature, flow and electron concentration fields, obtained for the cases (a)-(c). For all cases, the flowfield pattern is a typical backward facing step flow pattern influenced by Lorentz forces and centrifugal forces due to the swirling flow injection. It is

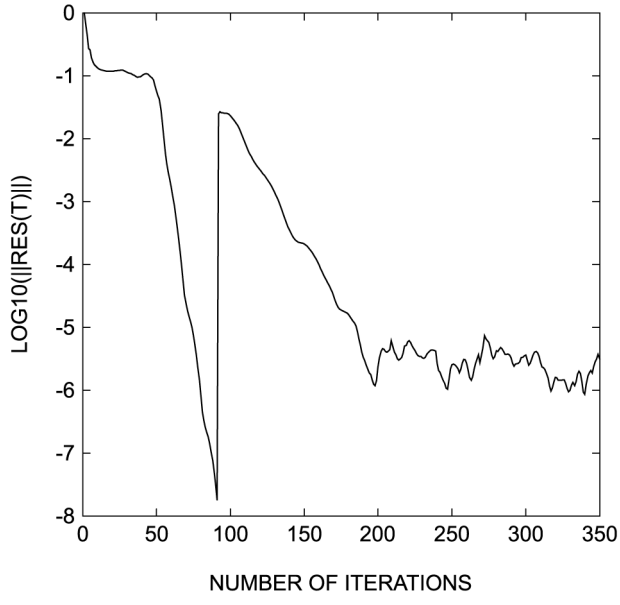

Figure 6.
Convergence histories of air ICP flow computations in the VKI Plasmatron torch

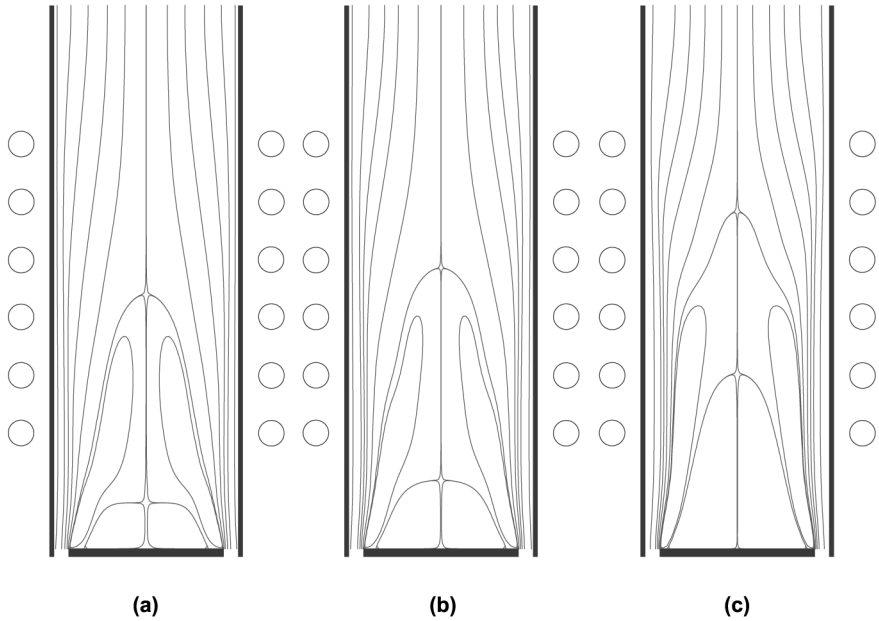

Figure 7.
Computed streamline patterns in the VKI Plasmatron torch: (a) LTE; (b) model of Selle and Riedel; and (c) model of Park

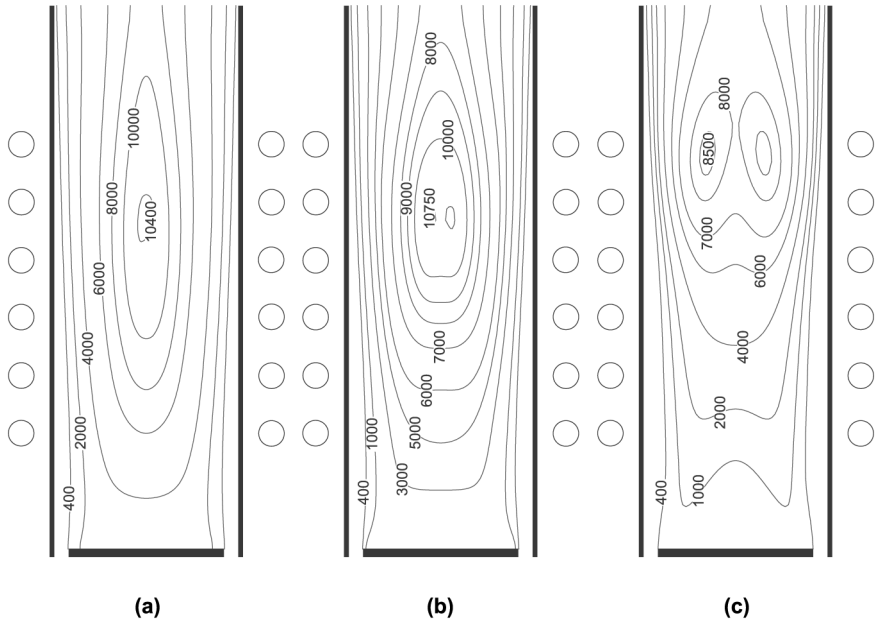

Figure 8.
Computed temperature contours in the VKI Plasmatron torch: (a) LTE; (b) model of Selle and Riedel; and (c) model of Park

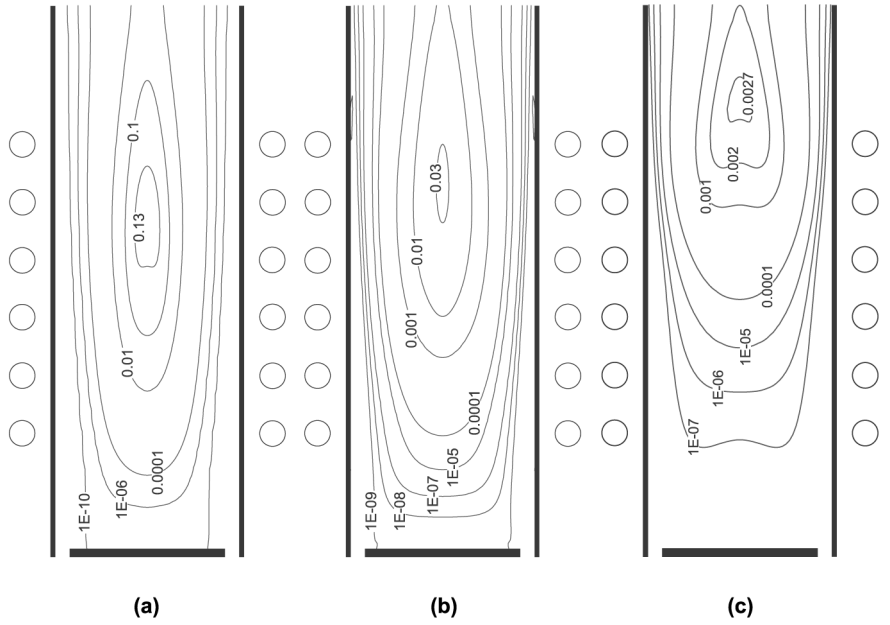

Figure 9.
Computed electron mole fraction contours in the VKI Plasmatron torch: (a) LTE; (b) model of Selle and Riedel; and (c) model of Park

seen that the non-equilibrium effects have a minor effect upon the obtained flow field.

Similar temperature fields with peak temperatures ~10,500 K on the axis are obtained when assuming LTE and when using the finite-rate chemistry model of Selle and Riedel (2000). However, important differences are observed in the corresponding electron concentration fields. As a result of convective quenching, the peak electron mole fraction ~0.03 found with the model of Selle and Riedel is more than four times smaller than the maximal LTE fraction ~0.13.

Far stronger non-equilibrium effects are found when using the model of Park (Gnoffo *et al.*, 1989). Peak temperatures ~8,500 K are found at a distinctive off-axis location. The maximal value of the electron mole fraction amounts to only ~0.003, which lies yet an order of magnitude beneath the value found using the model of Selle and Riedel. The fact that the peak in electron concentration does not coincide with the temperature maximum is entirely due to chemical non-equilibrium effects.

It should be noted that the temperatures and electron concentrations obtained when using Park's model are unrealistically low. In addition, the ionised gas itself lies behind the downstream end of the inductor, which indicates poor incoupling of energy. To obtain more physical results, thermal non-equilibrium effects should be added to the model. The temperature of free electrons rises faster than the equilibrium temperature used in our current simulations. Consequently, when a separate electron temperature is included,

the onset of ionisation will occur closer to the upstream end of the inductor and the overall degree of ionisation may be substantially higher.

7.4 Nuclei demixing

Figure 10 shows the computed contours of oxygen nuclei fractions (volumetric) obtained using the model of Selle and Riedel. It is seen that important demixing of oxygen and nitrogen elements occurs due to diffusive effects in the plasma. By multiplying the different species equations by the number of oxygen nuclei ξ_s^{O} in the respective species and summing over s, we obtain an advection-diffusion equation for the mass fraction of oxygen elements in the plasma:

$$\nabla\cdot\left[\rho\vec{u}\left(\sum_{s=1}^{n_s} y_s\xi_s^{\mathrm{O}}\right)\right]+\nabla\cdot\left[\sum_{s=1}^{n_s}\vec{J}_s\xi_s^{\mathrm{O}}\right]=0. \tag{27}$$

The right hand side of the above result is zero because no nuclei are created in chemical reactions. The absence of chemistry terms implies that demixing occurs even for plasmas under LTE. The assumption of constant nuclei fractions and vanishing nuclei fluxes, commonly used in LTE simulations of multi-component plasma flows (Vasil'evskii *et al.*, 1996) is therefore, not always justified. In general, the usual set of LTE flow field equations should be complemented with an advection-diffusion equation (27) for each element in the plasma.

8. Conclusions

In this paper, we have presented the model for high-pressure air ICPs developed at the von Karman Institute over the past few years. Great care has been taken to ensure good accuracy and efficiency of the model.

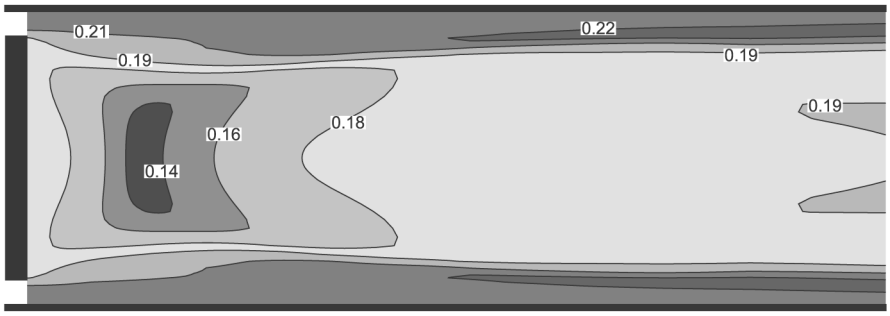

Figure 10.
Volumetric fraction of oxygen elements in the VKI Plasmatron torch (model of Selle and Riedel)

- Thermodynamic quantities are computed directly from statistical mechanics, using electronic cutoff criteria determined from systematic numerical experiments.
- Transport properties are computed from the Chapman-Enskog theory and validated mixture rules (two non-vanishing Sonine contributions are retained for electron properties).
- Diffusion fluxes in the poloidal plane are computed using the Stefan-Maxwell equations under the additional constraint of vanishing electric currents.
- The ICP model is based on the induction equation for the plasma-induced electric field only, which is solved for on a far-field mesh extending outside of the torch.
- The discrete equations are solved using efficient damped Picard and quasi-Newton techniques which allow fast computations of near equilibrium as well as non-equilibrium flows.

We have demonstrated the capabilities of the model by computing LTE and non-equilibrium air ICP flows inside the VKI Plasmatron torch. From the computed results, we may conclude the following.

- Chemical non-equilibrium effects may lead to significant deviations of LTE in the air ICPs typically used for TPM testing.
- The inadequacy of the air chemistry models currently available in the literature is clear, as very different results are obtained depending on the selected model.
- Inclusion of thermal NEQ effects is needed to obtain more physical results.
- Important demixing of oxygen and nitrogen nuclei occurs due to diffusion. As demixing takes place regardless of the degree of chemical non-equilibrium in the plasma, correct LTE models of chemically reacting viscous flows should include an additional advection-diffusion equation for each different element in the gas mixture.

It is clear that, before reliable quantitative predictions can be made, a very considerable effort remains to be invested in the development of a more adequate air chemistry model.

Note

1. There is actually one additional unknown (the total number of moles per unit volume) and one additional equation when solving for mole fractions.

References

Anderson, J.D. Jr (1989), *Hypersonics and High Temperature Gas Dynamics*, McGraw-Hill, New York, NY.

Benoy, D.A. (1993), "Modeling of thermal argon plasmas", PhD thesis, Technical University of Eindhoven, Eindhoven, The Netherlands.

Bottin, B. (1999) "Aerothermodynamic model of an inductively coupled plasma wind tunnel", PhD thesis, Université de Liège, Liège, Belgium.

Bottin, B., Chazot, O., Carbonaro, M., Van der Haegen, V. and Paris, S. (1999a), "The VKI Plasmatron characteristics and performance", in Charbonnier, J.M. and Sarma, G.S.R. (Eds), *Measurement Techniques for High Temperature and Plasma Flows*, NATO-RTO-EN 8.

Bottin, B., Vanden Abeele, D., Carbonaro, M., Degrez, G. and Sarma, G.S.R. (1999b), "Thermodynamic and transport properties for inductive plasma modelling", *Journal of Thermophysics and Heat Transfer*, Vol. 13 No. 3, pp. 343-50.

Butler, J.N. and Brokaw, R.S. (1957), "Thermal conductivity of gas mixtures, in chemical equilibrium", *Journal of Chemical Physics*, Vol. 26 No. 6, pp. 1636-43.

Devoto, R.S. (1967), "Simplified expression for the transport properties of ionized monoatomic gases", *Physics of fluids*, Vol. 10 No. 10, pp. 2105-12.

Drellishak, K.S., Aeschliman, D.P. and Cambel, A.B. (1965), "Partition functions and thermodynamic properties of nitrogen and oxygen plasmas", *Physics of Fluids*, Vol. 8 No. 9, pp. 1590-600.

Dresvin, S.V., Donskoi, A.V., Goldfarb, V.M. and Klubnikin, V.S. (1977) *Physics and Technology of Low-Temperature Plasmas*, in, Eckert, H.V. (Ed.), translated from Russian, Iowa State University Press, Ames, IA.

Ferziger, J.H. and Perić, M. (1996), *Computational Method for Fluid Dynamics*, Springer, Berlin.

Gnoffo, P.A., Gupta, R.N. and Shinn, J.L. (1989), "Conservation equations and physical models for hypersonic air flows in thermal and chemical nonequilibrium", *TP* 2867, NASA.

Gupta, R.N., Yos, J.M., Thompson, R.A. and Lee, K.P. (1990), "A review of reaction rates and thermodynamic and transport properties for an 11-species air model for chemical and thermal nonequilibrium calculations to 30,000 K", *RP* 1232, NASA.

Gurvich, L.V., Veyts, I.V. and Alcock, C.B. (1989), *Thermodynamic Properties of Individual Substances*, Part 2: Tables, Vol. 1, Hemisphere, New York, NY.

Hirsch, C. (1988), "Numierical computation of internal and external flows", *Computational Methods for Inviscid and Viscous Flows*, Vol. 2, Wiley, Chichester.

Hirschfelder, J.O., Curtiss, C.F. and Bird, R.B. (1967), *Molecular Theory of Gases and Liquids*, Wiley, New York, NY.

Jaeger, E.F., Berry, L.A., Tolliver, J.S. and Batchelor, D.B. (1995), "Power deposition in high-density inductively coupled plasma tools for semiconductor processing", *Physics of Plasmas*, Vol. 2 No. 6, pp. 2597-604.

Kolesnikov, A.F. (1999), "Combined measurements and computations of high enthalpy and plasma flows for determination of TPM surface catalycity", in Charbonnier, J.M. and Sarma, G.S.R. (Eds), *Measurement Techniques for High Temperature and Plasma Flows*, NATO-RTO-EN 8.

Kolesnikov, A.F. and Tirsky, G.A. (1984), "Hydrodynamics equations for partially ionised multicomponent gas mixtures with higher order approximations for transport coefficients", *Fluid Mechanics – Soviet Research*, Vol. 13 No. 4, pp. 70-97.

Kolesnikov, A.F., Pershin, I.S., Vasil'evskii, S.A. and Yakushin, M.I. (1998), "Study of quartz surface catalycity in dissociated carbon dioxide subsonic flows", AIAA Paper 98-2847.

Kulumbaev, E.B. (1999), "Development of thermochemical models of arc, induction, microwave and optical discharges", PhD thesis, Kyrgiz-Slavic University, Bishkek, Kyrgizstan (in Russian).

Mayer, J.E. and Mayer, M.G. (1946), *Statistical Mechanics*, Wiley, New York, NY.

Mekideche, M.R. (1993), "Contribution à la modélisation numérique de torches à plasma d'induction", PhD Thesis, École doctorale de Sicences pour, l'Ingénieur de Nantes, Saint-Nazaire, France.

Mostaghimi, J., Proulx, P. and Boulos, M.I. (1987), "A two-temperature model of the inductively coupled RF plasma", *Journal of Applied Physics*, Vol. 61 No. 5, pp. 1753-60.

Murphy, A.B. (1995), "Transport coefficients of air, argon-air, nitrogen-air and oxygen-air plasma", *Plasma Chemistry and Plasma Procession*, Vol. 15 No. 2, pp. 279-307.

Saad, Y. (1995), "Preconditioned Krylov subspace methods: an overview", in Hafez, M. and Oshima, K. (Eds), *Computational Fluid Dynamics Review*, Wiley, New York, NY.

Selle, S. and Riedel, U. (2000), "Transport coefficients of reacting air at high temperatures", *Technical Paper 2000-0211*, AIAA, Reno, Nevada.

Semin, V.A. (1991), "Theory of nonequilibrium inductive high-frequency discharge in a gas flow", *Mechanics of fluids and gases*, (translated from Russian), Vol. 26 No. 2, pp. 282-8.

Sutton, K. and Gnoffo, P. (1998), "Multi-component diffusion with application to computational aerothermodynamics", AIAA Paper 98-2575.

Van Dijk, J., van der Velden, M. and van der Mullen, J. (2002), "A multidomain boundary-relaxation technique for the calculation of the electromagnetic field in ferrite-code inductive plasmas", *Journal of Physics D: Applied Physics*, Vol. 35, pp. 2748-59.

Vanden Abeele, D. (2000), "An efficient computational model of inductively coupled air plasma flows under thermal and chemical non-equilibrium", PhD thesis, von Karman Institute for Fluid Dynamics/Katholieke Universiteit Leuven, Leuven, Belgium.

Vanden Abeele, D. and Degrez, G. (2000), "Efficient computational model for inductive plasma flows", *AIAA Journal*, Vol. 38 No. 2, pp. 234-42.

Vanden Abeele, D., Vasil'evskii, S.A., Kolesnikov, A.F., Degrez, G. and Bottin, B. (1999), "Code-to-code validation of inductive plasma computations", *VKI TN 197*, von Karman Institute for Fluid dynamics, St. Genesius-Rode, Belgium.

Vasil'evskii, S.A., Kolesnikov, A.F. and Yakushin, M.I. (1996), "Mathematical models for plasma and gas flows in induction plasmatrons", in Capitelli, M. (Ed.), *Molecular Physics and Hypersonic Flows*, Kluwer, Dordrecht, The Netherlands, pp. 495-504.

Vincenti, W.G. and Kruger, C.H. Jr (1965), *Introduction to Physical Gas Dynamics*, Wiley, New York, NY.

Yos, J.M. (1963), "Transport properties of nitrogen, hydrogen, oxygen and air to 30,000 K", RAD-TM-63-7, AVCO Corp., Wilmington, MA.